Measurement of Branching Fractions and Charge Asymmetries in B Decays to an η Meson and a K^* Meson

B. Aubert,[1] M. Bona,[1] D. Boutigny,[1] F. Couderc,[1] Y. Karyotakis,[1] J. P. Lees,[1] V. Poireau,[1] V. Tisserand,[1] A. Zghiche,[1] E. Grauges,[2] A. Palano,[3] J. C. Chen,[4] N. D. Qi,[4] G. Rong,[4] P. Wang,[4] Y. S. Zhu,[4] G. Eigen,[5] I. Ofte,[5] B. Stugu,[5] G. S. Abrams,[6] M. Battaglia,[6] D. N. Brown,[6] J. Button-Shafer,[6] R. N. Cahn,[6] E. Charles,[6] M. S. Gill,[6] Y. Groysman,[6] R. G. Jacobsen,[6] J. A. Kadyk,[6] L. T. Kerth,[6] Yu. G. Kolomensky,[6] G. Kukartsev,[6] G. Lynch,[6] L. M. Mir,[6] T. J. Orimoto,[6] M. Pripstein,[6] N. A. Roe,[6] M. T. Ronan,[6] W. A. Wenzel,[6] P. del Amo Sanchez,[7] M. Barrett,[7] K. E. Ford,[7] A. J. Hart,[7] T. J. Harrison,[7] C. M. Hawkes,[7] A. T. Watson,[7] T. Held,[8] H. Koch,[8] B. Lewandowski,[8] M. Pelizaeus,[8] K. Peters,[8] T. Schroeder,[8] M. Steinke,[8] J. T. Boyd,[9] J. P. Burke,[9] W. N. Cottingham,[9] D. Walker,[9] D. J. Asgeirsson,[10] T. Cuhadar-Donszelmann,[10] B. G. Fulsom,[10] C. Hearty,[10] N. S. Knecht,[10] T. S. Mattison,[10] J. A. McKenna,[10] A. Khan,[11] P. Kyberd,[11] M. Saleem,[11] D. J. Sherwood,[11] L. Teodorescu,[11] V. E. Blinov,[12] A. D. Bukin,[12] V. P. Druzhinin,[12] V. B. Golubev,[12] A. P. Onuchin,[12] S. I. Serednyakov,[12] Yu. I. Skovpen,[12] E. P. Solodov,[12] K. Yu Todyshev,[12] M. Bondioli,[13] M. Bruinsma,[13] M. Chao,[13] S. Curry,[13] I. Eschrich,[13] D. Kirkby,[13] A. J. Lankford,[13] P. Lund,[13] M. Mandelkern,[13] R. K. Mommsen,[13] W. Roethel,[13] D. P. Stoker,[13] S. Abachi,[14] C. Buchanan,[14] S. D. Foulkes,[15] J. W. Gary,[15] O. Long,[15] B. C. Shen,[15] K. Wang,[15] L. Zhang,[15] H. K. Hadavand,[16] E. J. Hill,[16] H. P. Paar,[16] S. Rahatlou,[16] V. Sharma,[16] J. W. Berryhill,[17] C. Campagnari,[17] A. Cunha,[17] B. Dahmes,[17] T. M. Hong,[17] D. Kovalskyi,[17] J. D. Richman,[17] T. W. Beck,[18] A. M. Eisner,[18] C. J. Flacco,[18] C. A. Heusch,[18] J. Kroseberg,[18] W. S. Lockman,[18] G. Nesom,[18] T. Schalk,[18] B. A. Schumm,[18] A. Seiden,[18] P. Spradlin,[18] D. C. Williams,[18] M. G. Wilson,[18] J. Albert,[19] E. Chen,[19] A. Dvoretskii,[19] F. Fang,[19] D. G. Hitlin,[19] I. Narsky,[19] T. Piatenko,[19] F. C. Porter,[19] A. Ryd,[19] G. Mancinelli,[20] B. T. Meadows,[20] K. Mishra,[20] M. D. Sokoloff,[20] F. Blanc,[21] P. C. Bloom,[21] S. Chen,[21] W. T. Ford,[21] J. F. Hirschauer,[21] A. Kreisel,[21] M. Nagel,[21] U. Nauenberg,[21] A. Olivas,[21] W. O. Ruddick,[21] J. G. Smith,[21] K. A. Ulmer,[21] S. R. Wagner,[21] J. Zhang,[21] A. Chen,[22] E. A. Eckhart,[22] A. Soffer,[22] W. H. Toki,[22] R. J. Wilson,[22] F. Winklmeier,[22] Q. Zeng,[22] D. D. Altenburg,[23] E. Feltresi,[23] A. Hauke,[23] H. Jasper,[23] J. Merkel,[23] A. Petzold,[23] B. Spaan,[23] T. Brandt,[24] V. Klose,[24] H. M. Lacker,[24] W. F. Mader,[24] R. Nogowski,[24] J. Schubert,[24] K. R. Schubert,[24] R. Schwierz,[24] J. E. Sundermann,[24] A. Volk,[24] D. Bernard,[25] G. R. Bonneaud,[25] E. Latour,[25] Ch. Thiebaux,[25] M. Verderi,[25] P. J. Clark,[26] W. Gradl,[26] F. Muheim,[26] S. Playfer,[26] A. I. Robertson,[26] Y. Xie,[26] M. Andreotti,[27] D. Bettoni,[27] C. Bozzi,[27] R. Calabrese,[27] G. Cibinetto,[27] E. Luppi,[27] M. Negrini,[27] A. Petrella,[27] L. Piemontese,[27] E. Prencipe,[27] F. Anulli,[28] R. Baldini-Ferroli,[28] A. Calcaterra,[28] R. de Sangro,[28] G. Finocchiaro,[28] S. Pacetti,[28] P. Patteri,[28] I. M. Peruzzi,[28,*] M. Piccolo,[28] M. Rama,[28] A. Zallo,[28] A. Buzzo,[29] R. Contri,[29] M. Lo Vetere,[29] M. M. Macri,[29] M. R. Monge,[29] S. Passaggio,[29] C. Patrignani,[29] E. Robutti,[29] A. Santroni,[29] S. Tosi,[29] G. Brandenburg,[30] K. S. Chaisanguanthum,[30] M. Morii,[30] J. Wu,[30] R. S. Dubitzky,[31] J. Marks,[31] S. Schenk,[31] U. Uwer,[31] D. J. Bard,[32] W. Bhimji,[32] D. A. Bowerman,[32] P. D. Dauncey,[32] U. Egede,[32] R. L. Flack,[32] J. A. Nash,[32] M. B. Nikolich,[32] W. Panduro Vazquez,[32] D. J. Bard,[33] P. K. Behera,[33] X. Chai,[33] M. J. Charles,[33] U. Mallik,[33] N. T. Meyer,[33] V. Ziegler,[33] J. Cochran,[34] H. B. Crawley,[34] L. Dong,[34] V. Eyges,[34] W. T. Meyer,[34] S. Prell,[34] E. I. Rosenberg,[34] A. E. Rubin,[34] A. V. Gritsan,[35] A. G. Denig,[36] M. Fritsch,[36] G. Schott,[36] N. Arnaud,[37] M. Davier,[37] G. Grosdidier,[37] A. Höcker,[37] F. Le Diberder,[37] V. Lepeltier,[37] A. M. Lutz,[37] A. Oyanguren,[37] S. Pruvot,[37] S. Rodier,[37] P. Roudeau,[37] M. H. Schune,[37] A. Stocchi,[37] W. F. Wang,[37] G. Wormser,[37] C. H. Cheng,[38] D. J. Lange,[38] D. M. Wright,[38] C. A. Chavez,[39] I. J. Forster,[39] J. R. Fry,[39] E. Gabathuler,[39] R. Gamet,[39] K. A. George,[39] D. E. Hutchcroft,[39] D. J. Payne,[39] K. C. Schofield,[39] C. Touramanis,[39] A. J. Bevan,[40] F. Di Lodovico,[40] W. Menges,[40] R. Sacco,[40] G. Cowan,[41] H. U. Flaecher,[41] D. A. Hopkins,[41] P. S. Jackson,[41] T. R. McMahon,[41] S. Ricciardi,[41] F. Salvatore,[41] A. C. Wren,[41] D. N. Brown,[42] C. L. Davis,[42] J. Allison,[43] N. R. Barlow,[43] R. J. Barlow,[43] Y. M. Chia,[43] C. L. Edgar,[43] G. D. Lafferty,[43] M. T. Naisbit,[43] J. C. Williams,[43] J. I. Yi,[43] C. Chen,[44] W. D. Hulsbergen,[44] A. Jawahery,[44] C. K. Lae,[44] D. A. Roberts,[44] G. Simi,[44] G. Blaylock,[45] C. Dallapiccola,[45] S. S. Hertzbach,[45] X. Li,[45] T. B. Moore,[45] S. Saremi,[45] H. Staengle,[45] R. Cowan,[46] G. Sciolla,[46] S. J. Sekula,[46] M. Spitznagel,[46] F. Taylor,[46] R. K. Yamamoto,[46] H. Kim,[47] S. E. Mclachlin,[47] P. M. Patel,[47] S. H. Robertson,[47] A. Lazzaro,[48] V. Lombardo,[48] F. Palombo,[48] J. M. Bauer,[49] L. Cremaldi,[49] V. Eschenburg,[49] R. Godang,[49] R. Kroeger,[49] D. A. Sanders,[49] D. J. Summers,[49] H. W. Zhao,[49] S. Brunet,[50] D. Côté,[50] M. Simard,[50] P. Taras,[50] F. B. Viaud,[50] H. Nicholson,[51] N. Cavallo,[52,†] G. De Nardo,[52] F. Fabozzi,[52,†] C. Gatto,[52] L. Lista,[52] D. Monorchio,[52] P. Paolucci,[52] D. Piccolo,[52] C. Sciacca,[52] M. A. Baak,[53] G. Raven,[53] H. L. Snoek,[53] C. P. Jessop,[54] J. M. LoSecco,[54] T. Allmendinger,[55] G. Benelli,[55] L. A. Corwin,[55] K. K. Gan,[55] K. Honscheid,[55] D. Hufnagel,[55] P. D. Jackson,[55] H. Kagan,[55] R. Kass,[55] A. M. Rahimi,[55] J. J. Regensburger,[55] R. Ter-Antonyan,[55] Q. K. Wong,[55]

N. L. Blount,[56] J. Brau,[56] R. Frey,[56] O. Igonkina,[56] J. A. Kolb,[56] M. Lu,[56] R. Rahmat,[56] N. B. Sinev,[56] D. Strom,[56] J. Strube,[56] E. Torrence,[56] A. Gaz,[57] M. Margoni,[57] M. Morandin,[57] A. Pompili,[57] M. Posocco,[57] M. Rotondo,[57] F. Simonetto,[57] R. Stroili,[57] C. Voci,[57] M. Benayoun,[58] H. Briand,[58] J. Chauveau,[58] P. David,[58] L. Del Buono,[58] Ch. de la Vaissière,[58] O. Hamon,[58] B. L. Hartfiel,[58] Ph. Leruste,[58] J. Malclès,[58] J. Ocariz,[58] L. Roos,[58] G. Therin,[58] L. Gladney,[59] M. Biasini,[60] R. Covarelli,[60] C. Angelini,[61] G. Batignani,[61] S. Bettarini,[61] F. Bucci,[61] G. Calderini,[61] M. Carpinelli,[61] R. Cenci,[61] F. Forti,[61] M. A. Giorgi,[61] A. Lusiani,[61] G. Marchiori,[61] M. A. Mazur,[61] M. Morganti,[61] N. Neri,[61] E. Paoloni,[61] G. Rizzo,[61] J. J. Walsh,[61] M. Haire,[62] D. Judd,[62] D. E. Wagoner,[62] J. Biesiada,[63] N. Danielson,[63] P. Elmer,[63] Y. P. Lau,[63] C. Lu,[63] J. Olsen,[63] A. J. S. Smith,[63] A. V. Telnov,[63] F. Bellini,[64] G. Cavoto,[64] A. D'Orazio,[64] D. del Re,[64] E. Di Marco,[64] R. Faccini,[64] F. Ferrarotto,[64] F. Ferroni,[64] M. Gaspero,[64] L. Li Gioi,[64] M. A. Mazzoni,[64] S. Morganti,[64] G. Piredda,[64] F. Polci,[64] F. Safai Tehrani,[64] C. Voena,[64] M. Ebert,[65] H. Schröder,[65] R. Waldi,[65] T. Adye,[66] N. De Groot,[66] B. Franek,[66] E. O. Olaiya,[66] F. F. Wilson,[66] R. Aleksan,[67] S. Emery,[67] A. Gaidot,[67] S. F. Ganzhur,[67] G. Hamel de Monchenault,[67] W. Kozanecki,[67] M. Legendre,[67] G. Vasseur,[67] Ch. Yèche,[67] M. Zito,[67] X. R. Chen,[68] H. Liu,[68] W. Park,[68] M. V. Purohit,[68] J. R. Wilson,[68] M. T. Allen,[69] D. Aston,[69] R. Bartoldus,[69] P. Bechtle,[69] N. Berger,[69] R. Claus,[69] J. P. Coleman,[69] M. R. Convery,[69] M. Cristinziani,[69] J. C. Dingfelder,[69] J. Dorfan,[69] G. P. Dubois-Felsmann,[69] D. Dujmic,[69] W. Dunwoodie,[69] R. C. Field,[69] T. Glanzman,[69] S. J. Gowdy,[69] M. T. Graham,[69] P. Grenier,[69] V. Halyo,[69] C. Hast,[69] T. Hryn'ova,[69] W. R. Innes,[69] M. H. Kelsey,[69] P. Kim,[69] D. W. G. S. Leith,[69] S. Li,[69] S. Luitz,[69] V. Luth,[69] H. L. Lynch,[69] D. B. MacFarlane,[69] H. Marsiske,[69] R. Messner,[69] D. R. Muller,[69] C. P. O'Grady,[69] V. E. Ozcan,[69] A. Perazzo,[69] M. Perl,[69] T. Pulliam,[69] B. N. Ratcliff,[69] A. Roodman,[69] A. A. Salnikov,[69] R. H. Schindler,[69] J. Schwiening,[69] A. Snyder,[69] J. Stelzer,[69] D. Su,[69] M. K. Sullivan,[69] K. Suzuki,[69] S. K. Swain,[69] J. M. Thompson,[69] J. Va'vra,[69] N. van Bakel,[69] M. Weaver,[69] A. J. R. Weinstein,[69] W. J. Wisniewski,[69] M. Wittgen,[69] D. H. Wright,[69] A. K. Yarritu,[69] K. Yi,[69] C. C. Young,[69] P. R. Burchat,[70] A. J. Edwards,[70] S. A. Majewski,[70] B. A. Petersen,[70] C. Roat,[70] L. Wilden,[70] S. Ahmed,[71] M. S. Alam,[71] R. Bula,[71] J. A. Ernst,[71] V. Jain,[71] B. Pan,[71] M. A. Saeed,[71] F. R. Wappler,[71] S. B. Zain,[71] W. Bugg,[72] M. Krishnamurthy,[72] S. M. Spanier,[72] R. Eckmann,[73] J. L. Ritchie,[73] A. Satpathy,[73] C. J. Schilling,[73] R. F. Schwitters,[73] J. M. Izen,[74] X. C. Lou,[74] S. Ye,[74] F. Bianchi,[75] F. Gallo,[75] D. Gamba,[75] M. Bomben,[76] L. Bosisio,[76] C. Cartaro,[76] F. Cossutti,[76] G. Della Ricca,[76] S. Dittongo,[76] L. Lanceri,[76] L. Vitale,[76] V. Azzolini,[77] N. Lopez-March,[77] F. Martinez-Vidal,[77] Sw. Banerjee,[78] B. Bhuyan,[78] C. M. Brown,[78] D. Fortin,[78] K. Hamano,[78] R. Kowalewski,[78] I. M. Nugent,[78] J. M. Roney,[78] R. J. Sobie,[78] J. J. Back,[79] P. F. Harrison,[79] T. E. Latham,[79] G. B. Mohanty,[79] M. Pappagallo,[79] H. R. Band,[80] X. Chen,[80] B. Cheng,[80] S. Dasu,[80] M. Datta,[80] K. T. Flood,[80] J. J. Hollar,[80] P. E. Kutter,[80] B. Mellado,[80] A. Mihalyi,[80] Y. Pan,[80] M. Pierini,[80] R. Prepost,[80] S. L. Wu,[80] Z. Yu,[80] and H. Neal[81]

(*BABAR* Collaboration)

[1]*Laboratoire de Physique des Particules, IN2P3/CNRS et Université de Savoie, F-74941 Annecy-Le-Vieux, France*
[2]*Universitat de Barcelona, Facultat de Fisica, Departament ECM, E-08028 Barcelona, Spain*
[3]*Università di Bari, Dipartimento di Fisica and INFN, I-70126 Bari, Italy*
[4]*Institute of High Energy Physics, Beijing 100039, China*
[5]*University of Bergen, Institute of Physics, N-5007 Bergen, Norway*
[6]*Lawrence Berkeley National Laboratory and University of California, Berkeley, California 94720, USA*
[7]*University of Birmingham, Birmingham, B15 2TT, United Kingdom*
[8]*Ruhr Universität Bochum, Institut für Experimentalphysik 1, D-44780 Bochum, Germany*
[9]*University of Bristol, Bristol BS8 1TL, United Kingdom*
[10]*University of British Columbia, Vancouver, British Columbia, Canada V6T 1Z1*
[11]*Brunel University, Uxbridge, Middlesex UB8 3PH, United Kingdom*
[12]*Budker Institute of Nuclear Physics, Novosibirsk 630090, Russia*
[13]*University of California at Irvine, Irvine, California 92697, USA*
[14]*University of California at Los Angeles, Los Angeles, California 90024, USA*
[15]*University of California at Riverside, Riverside, California 92521, USA*
[16]*University of California at San Diego, La Jolla, California 92093, USA*
[17]*University of California at Santa Barbara, Santa Barbara, California 93106, USA*
[18]*University of California at Santa Cruz, Institute for Particle Physics, Santa Cruz, California 95064, USA*
[19]*California Institute of Technology, Pasadena, California 91125, USA*
[20]*University of Cincinnati, Cincinnati, Ohio 45221, USA*
[21]*University of Colorado, Boulder, Colorado 80309, USA*
[22]*Colorado State University, Fort Collins, Colorado 80523, USA*
[23]*Universität Dortmund, Institut für Physik, D-44221 Dortmund, Germany*

[24]Technische Universität Dresden, Institut für Kern- und Teilchenphysik, D-01062 Dresden, Germany
[25]Laboratoire Leprince-Ringuet, CNRS/IN2P3, Ecole Polytechnique, F-91128 Palaiseau, France
[26]University of Edinburgh, Edinburgh EH9 3JZ, United Kingdom
[27]Università di Ferrara, Dipartimento di Fisica and INFN, I-44100 Ferrara, Italy
[28]Laboratori Nazionali di Frascati dell'INFN, I-00044 Frascati, Italy
[29]Università di Genova, Dipartimento di Fisica and INFN, I-16146 Genova, Italy
[30]Harvard University, Cambridge, Massachusetts 02138, USA
[31]Universität Heidelberg, Physikalisches Institut, Philosophenweg 12, D-69120 Heidelberg, Germany
[32]Imperial College London, London, SW7 2AZ, United Kingdom
[33]University of Iowa, Iowa City, Iowa 52242, USA
[34]Iowa State University, Ames, Iowa 50011-3160, USA
[35]Johns Hopkins University, Baltimore, Maryland 21218, USA
[36]Universität Karlsruhe, Institut für Experimentelle Kernphysik, D-76021 Karlsruhe, Germany
[37]Laboratoire de l'Accélérateur Linéaire, IN2P3/CNRS et Université Paris-Sud 11, Centre Scientifique d'Orsay, B.P. 34, F-91898 ORSAY Cedex, France
[38]Lawrence Livermore National Laboratory, Livermore, California 94550, USA
[39]University of Liverpool, Liverpool L69 7ZE, United Kingdom
[40]Queen Mary, University of London, E1 4NS, United Kingdom
[41]University of London, Royal Holloway and Bedford New College, Egham, Surrey TW20 0EX, United Kingdom
[42]University of Louisville, Louisville, Kentucky 40292, USA
[43]University of Manchester, Manchester M13 9PL, United Kingdom
[44]University of Maryland, College Park, Maryland 20742, USA
[45]University of Massachusetts, Amherst, Massachusetts 01003, USA
[46]Massachusetts Institute of Technology, Laboratory for Nuclear Science, Cambridge, Massachusetts 02139, USA
[47]McGill University, Montréal, Québec, Canada H3A 2T8
[48]Università di Milano, Dipartimento di Fisica and INFN, I-20133 Milano, Italy
[49]University of Mississippi, University, Mississippi 38677, USA
[50]Université de Montréal, Physique des Particules, Montréal, Québec, Canada H3C 3J7
[51]Mount Holyoke College, South Hadley, Massachusetts 01075, USA
[52]Università di Napoli Federico II, Dipartimento di Scienze Fisiche and INFN, I-80126, Napoli, Italy
[53]NIKHEF, National Institute for Nuclear Physics and High Energy Physics, NL-1009 DB Amsterdam, The Netherlands
[54]University of Notre Dame, Notre Dame, Indiana 46556, USA
[55]The Ohio State University, Columbus, Ohio 43210, USA
[56]University of Oregon, Eugene, Oregon 97403, USA
[57]Università di Padova, Dipartimento di Fisica and INFN, I-35131 Padova, Italy
[58]Laboratoire de Physique Nucléaire et de Hautes Energies, IN2P3/CNRS, Université Pierre et Marie Curie-Paris6, Université Denis Diderot-Paris7, F-75252 Paris, France
[59]University of Pennsylvania, Philadelphia, Pennsylvania 19104, USA
[60]Università di Perugia, Dipartimento di Fisica and INFN, I-06100 Perugia, Italy
[61]Università di Pisa, Dipartimento di Fisica, Scuola Normale Superiore and INFN, I-56127 Pisa, Italy
[62]Prairie View A&M University, Prairie View, Texas 77446, USA
[63]Princeton University, Princeton, New Jersey 08544, USA
[64]Università di Roma La Sapienza, Dipartimento di Fisica and INFN, I-00185 Roma, Italy
[65]Universität Rostock, D-18051 Rostock, Germany
[66]Rutherford Appleton Laboratory, Chilton, Didcot, Oxon, OX11 0QX, United Kingdom
[67]DSM/Dapnia, CEA/Saclay, F-91191 Gif-sur-Yvette, France
[68]University of South Carolina, Columbia, South Carolina 29208, USA
[69]Stanford Linear Accelerator Center, Stanford, California 94309, USA
[70]Stanford University, Stanford, California 94305-4060, USA
[71]State University of New York, Albany, New York 12222, USA
[72]University of Tennessee, Knoxville, Tennessee 37996, USA
[73]University of Texas at Austin, Austin, Texas 78712, USA
[74]University of Texas at Dallas, Richardson, Texas 75083, USA
[75]Università di Torino, Dipartimento di Fisica Sperimentale and INFN, I-10125 Torino, Italy
[76]Università di Trieste, Dipartimento di Fisica and INFN, I-34127 Trieste, Italy
[77]IFIC, Universitat de Valencia–CSIC, E-46071 Valencia, Spain
[78]University of Victoria, Victoria, British Columbia, Canada V8W 3P6
[79]Department of Physics, University of Warwick, Coventry CV4 7AL, United Kingdom
[80]University of Wisconsin, Madison, Wisconsin 53706, USA
[81]Yale University, New Haven, Connecticut 06511, USA

(Received 2 August 2006; published 15 November 2006)

We present measurements of branching fractions and charge asymmetries for the decays $B \to \eta K^*$, where K^* indicates a spin 0, 1, or 2 $K\pi$ system. The data sample corresponds to 344×10^6 $B\bar{B}$ pairs collected with the *BABAR* detector at the PEP-II asymmetric-energy e^+e^- collider at SLAC. We measure the branching fractions (in units of 10^{-6}): $\mathcal{B}(B^0 \to \eta K^{*0}(892)) = 16.5 \pm 1.1 \pm 0.8$, $\mathcal{B}(B^+ \to \eta K^{*+}(892)) = 18.9 \pm 1.8 \pm 1.3$, $\mathcal{B}(B^0 \to \eta(K\pi)^{*0}_0) = 11.0 \pm 1.6 \pm 1.5$, $\mathcal{B}(B^+ \to \eta(K\pi)^{*+}_0) = 18.2 \pm 2.6 \pm 2.6$, $\mathcal{B}(B^0 \to \eta K^{*0}_2(1430)) = 9.6 \pm 1.8 \pm 1.1$, and $\mathcal{B}(B^+ \to \eta K^{*+}_2(1430)) = 9.1 \pm 2.7 \pm 1.4$. We also determine the charge asymmetries for all decay modes.

DOI: 10.1103/PhysRevLett.97.201802 PACS numbers: 13.25.Hw, 11.30.Er

Decays of B mesons to charmless hadronic final states are widely used to test the accuracy of theoretical predictions. The decays involving η and η' mesons have received considerable attention because early predictions were unable to explain the data. For decays of interest in this paper, there have been recent calculations from QCD factorization [1,2] and flavor SU(3) symmetry [3].

Charmless B decays to final states with strangeness are expected to be dominated by $b \to s$ loop ("penguin") amplitudes. The branching fraction for the decay $B \to \eta K^*$ is expected to be larger than most similar decays (though not as large as $B \to \eta' K$) due to constructive interference between two penguin amplitudes [4].

While the decay $B \to \eta K^*(892)$ has been seen previously [5,6], there have been no searches for states with an η meson accompanied by $K^*(1430)$ mesons, and no theoretical predictions exist for these decays. In this Letter we present measurements of branching fractions and charge asymmetries for the decays $B^0 \to \eta K^{*0}(892)$ [7], $B^+ \to \eta K^{*+}(892)$, $B^0 \to \eta(K\pi)^{*0}_0$, $B^+ \to \eta(K\pi)^{*+}_0$, $B^0 \to \eta K^{*0}_2(1430)$, and $B^+ \to \eta K^{*+}_2(1430)$, where we denote by $(K\pi)^*_0$ the 0^+ component of the $K\pi$ spectrum. The charge asymmetry is defined as $\mathcal{A}_{\rm ch} \equiv (\Gamma^- - \Gamma^+)/(\Gamma^- + \Gamma^+)$, where the superscript on the width Γ corresponds to the sign of the $B^\pm$ meson or the sign of the charged kaon for B^0 decays.

The results presented here are obtained from data collected with the *BABAR* detector (described in detail elsewhere [8]) at the PEP-II asymmetric e^+e^- collider located at the Stanford Linear Accelerator Center. The analysis uses an integrated luminosity of 313 fb^{-1}, corresponding to 344×10^6 $B\bar{B}$ pairs, recorded at the $\Upsilon(4S)$ resonance [center-of-mass (CM) energy $\sqrt{s} = 10.58$ GeV], and follows closely the technique described in detail in Ref. [6]. The sample is 3.9 times larger than that of Ref. [6].

The K^* mesons are reconstructed from $K^+\pi^0$ ($K^{*+}_{K^+\pi^0}$), $K^0_S\pi^+$ ($K^{*+}_{K^0_S}\pi^+$), or $K^+\pi^-$ ($K^{*0}_{K^+\pi^-}$) final states. All tracks from resonance candidates are required to have charged particle identification (PID) consistent with kaons or pions. We select η, K^0_S, and π^0 candidates from the decays $\eta \to \gamma\gamma$ ($\eta_{\gamma\gamma}$), $\eta \to \pi^+\pi^-\pi^0$ ($\eta_{3\pi}$), $K^0_S \to \pi^+\pi^-$, and $\pi^0 \to \gamma\gamma$. We impose the following requirements on the invariant masses (in MeV) of the particle candidate final states: $490 < m_{\gamma\gamma} < 600$ for $\eta_{\gamma\gamma}$, $520 < m_{\pi\pi\pi} < 570$ for $\eta_{3\pi}$, $486 < m_{\pi\pi} < 510$ for K^0_S, and $120 < m_{\gamma\gamma} < 150$ for π^0. For K^0_S candidates we require at least 3 standard-deviation (σ) three-dimensional separation between the decay vertex and the e^+e^- collision point. Requirements are loose for the variables used in the maximum likelihood (ML) fit described below. For the $K\pi$ system, we define a low-mass region (LMR) by $755 < m_{K\pi} < 1035$ MeV and a high-mass region (HMR) by $1035 < m_{K\pi} < 1535$ MeV [9]. For the K^* we use the helicity frame, defined as the K^* rest frame with polar axis opposite to the direction of the B. We define $\mathcal{H} \equiv \cos\theta_H$, where the decay angle θ_H is the polar angle of the kaon momentum in the helicity frame. For the LMR, we require $-0.95 < \mathcal{H} < 1.0$ for K^{*0} and $K^{*+}_{K^0_S}\pi^+$, and $-0.7 < \mathcal{H} < 1.0$ for $K^{*+}_{K^+\pi^0}$. For the HMR, we require $-0.5 < \mathcal{H} < 1.0$ for all modes in order to remove the region in $\mathcal{H}$ having very large backgrounds.

A B-meson candidate is characterized kinematically by the energy-substituted mass $m_{\rm ES} = (\frac{1}{4}s - \mathbf{p}_B^2)^{1/2}$ and energy difference $\Delta E = E_B - \frac{1}{2}\sqrt{s}$, where $(E_B, \mathbf{p}_B)$ is the B-meson four-momentum vector, and all values are expressed in the $\Upsilon(4S)$ frame. Signal events peak at zero for ΔE, and at the B mass [10] for $m_{\rm ES}$, with a resolution for ΔE ($m_{\rm ES}$) of 30–45 MeV (3.0 MeV). We require $|\Delta E| \leq 0.2$ GeV and $5.25 \leq m_{\rm ES} < 5.29$ GeV.

The angle θ_T between the thrust axis of the B candidate in the $\Upsilon(4S)$ frame and that of the rest of the charged tracks and neutral clusters in the event is used to reject the dominant continuum $e^+e^- \to q\bar{q}$ ($q = u, d, s, c$) background events. The distribution of $|\cos\theta_T|$ is sharply peaked near 1.0 for combinations drawn from jetlike $q\bar{q}$ pairs, and nearly uniform for the almost isotropic B-meson decays; we require $|\cos\theta_T| \leq 0.9$. Further discrimination from continuum in the ML fit is obtained from energy flow in the event via a Fisher discriminant $\mathcal{F}$ that is described in detail elsewhere [6].

For the modes with $\eta \to \gamma\gamma$, we reject $B \to K^*\gamma$ background with the requirement $|\cos\theta^\eta_{\rm dec}| \leq 0.86$, where $\theta^\eta_{\rm dec}$ is the η decay angle defined, in the η rest frame, as the angle between one of the photons and the B direction.

When there are multiple candidates (fewer than 30% of events [9]), we choose the candidate with a value of the reconstructed η mass closest to the Particle Data Group mass [10].

We use Monte Carlo (MC) simulations [11] for the few charmless $B\bar{B}$ background decays that survive the candidate selection and have characteristics similar to the signal. We find these contributions to be negligible for all modes with an $\eta \to \pi^+\pi^-\pi^0$ decay except $\eta_{3\pi}K^{*0}$. For all other modes, we include a component in the ML fit to account for them.

We obtain yields and $\mathcal{A}_{\rm ch}$ for each decay chain from an extended unbinned maximum likelihood fit with the following input observables: ΔE, $m_{\rm ES}$, $\mathcal{F}$, $m_{\rm res}$ (the masses of the η and K^* candidates), and $\mathcal{H}$. For each event i and hypothesis j (signal, continuum background, $B\bar{B}$ background), we define the probability density function (PDF), with resulting likelihood $\mathcal{L}$ as follows:

$$\mathcal{P}_j^i = \mathcal{P}_j(m_{\rm ES}^i)\mathcal{P}_j(\Delta E^i)\mathcal{P}_j(\mathcal{F}^i)\mathcal{P}_j(m_{\rm res}^i)\mathcal{P}_j(\mathcal{H}^i) \quad (1)$$

$$\mathcal{L} = \exp\left(-\sum_j Y_j\right)\prod_i^N\left[\sum_j Y_j\mathcal{P}_j^i\right], \quad (2)$$

where Y_j is the yield of events of hypothesis j, and N is the number of events in the sample. The free parameters of the fit are the signal and background yields, between 9 and 11 $q\bar{q}$ background PDF parameters (see below), and the signal and $q\bar{q}$ background charge asymmetries.

We determine the contributions from $K^*(892)$, $(K\pi)_0^*$, and $K_2^*(1430)$ by fits in the LMR and HMR. The fit in the LMR includes $K^*(892)$ and $(K\pi)_0^*$ signal components [$K_2^*(1430)$ is negligible in this region], with the fixed $(K\pi)_0^*$ yield determined from the result of the fit to the HMR. For the fit in the HMR, all three components are included; the $K^*(892)$ yield is fixed from the result of the fit in the LMR, while the $(K\pi)_0^*$ and $K_2^*(1430)$ branching fractions are free in a simultaneous fit over the two (four) subdecay modes for K^{*0} (K^{*+}). For the generated $(K\pi)_0^*$ spectrum, we use a LASS model [12] which consists of the $K_0^*(1430)$ resonance together with an effective-range non-

TABLE I. Fitted signal yield Y_S in events (ev), measured bias (see text), detection efficiency ϵ, daughter branching fraction product ($\prod \mathcal{B}_i$), significance $\mathcal{S}$ (with systematic uncertainties included), measured branching fraction $\mathcal{B}$, and signal charge asymmetry $\mathcal{A}_{\rm ch}$ for each mode. The results of combining submodes are shown in bold face, where the first uncertainty is statistical and the second systematic.

Mode	Y_S (ev)	Bias (ev)	ϵ (%)	$\prod \mathcal{B}_i$ (%)	$\mathcal{S}$ (σ)	$\mathcal{B}$ (10^{-6})	$\mathcal{A}_{\rm ch}$
$\eta_{\gamma\gamma}K^{*0}_{K^+\pi^-}(892)$	407 ± 29	$+15$	24	26	17.6	18.2 ± 1.4	0.24 ± 0.07
$\eta_{3\pi}K^{*0}_{K^+\pi^-}(892)$	111 ± 16	$+13$	16	15	6.3	10.9 ± 2.0	0.12 ± 0.14
$B^0 \to \eta K^{*0}(892)$					**18.8**	$\mathbf{16.5 \pm 1.1 \pm 0.8}$	$\mathbf{0.21 \pm 0.06 \pm 0.02}$
$\eta_{\gamma\gamma}K^{*+}_{K^+\pi^0}(892)$	99 ± 16	$+7$	11	13	6.9	18.0 ± 3.2	0.19 ± 0.16
$\eta_{3\pi}K^{*+}_{K^+\pi^0}(892)$	56 ± 11	$+4$	8	8	6.1	25.4 ± 5.5	-0.05 ± 0.20
$\eta_{\gamma\gamma}K^{*+}_{K^0_S\pi^+}(892)$	149 ± 19	$+12$	22	9	8.6	20.5 ± 2.9	-0.03 ± 0.13
$\eta_{3\pi}K^{*+}_{K^0_S\pi^+}(892)$	36 ± 10	$+5$	15	5	3.8	11.9 ± 3.9	-0.23 ± 0.28
$B^+ \to \eta K^{*+}(892)$					**13.0**	$\mathbf{18.9 \pm 1.8 \pm 1.3}$	$\mathbf{0.01 \pm 0.08 \pm 0.02}$
$\eta_{\gamma\gamma}K_0^{*0}(K^+\pi^-)$	163 ± 25	$+17$	15	26	5.3	10.8 ± 1.9	0.14 ± 0.15
$\eta_{3\pi}K_0^{*0}(K^+\pi^-)$	69 ± 17	$+9$	10	15	3.6	11.4 ± 3.2	-0.18 ± 0.25
$B^0 \to \eta(K\pi)_0^{*0}$					**5.7**	$\mathbf{11.0 \pm 1.6 \pm 1.5}$	$\mathbf{0.06 \pm 0.13 \pm 0.02}$
$\eta_{\gamma\gamma}K_0^{*+}(K^+\pi^0)$	93 ± 20	$+9$	10	13	4.3	19.2 ± 4.5	-0.05 ± 0.21
$\eta_{3\pi}K_0^{*+}(K^+\pi^0)$	39 ± 12	$+6$	7	8	3.4	18.0 ± 6.3	0.03 ± 0.29
$\eta_{\gamma\gamma}K_0^{*+}(K^0_S\pi^0)$	55 ± 16	$+5$	12	9	3.0	13.3 ± 4.2	0.13 ± 0.25
$\eta_{3\pi}K_0^{*+}(K^0_S\pi^+)$	49 ± 11	$+3$	9	5	4.4	28.1 ± 6.7	0.18 ± 0.22
$B^+ \to \eta(K\pi)_0^{*+}$					**5.9**	$\mathbf{18.2 \pm 2.6 \pm 2.6}$	$\mathbf{0.05 \pm 0.13 \pm 0.02}$
$\eta_{\gamma\gamma}K_2^{*0}(K^+\pi^-)$	72 ± 17	-1	18	14	4.7	8.4 ± 1.9	-0.20 ± 0.23
$\eta_{3\pi}K_2^{*0}(K^+\pi^-)$	40 ± 13	-1	12	8	3.4	12.5 ± 4.1	0.23 ± 0.31
$B^0 \to \eta K_2^{*0}(1430)$					**5.3**	$\mathbf{9.6 \pm 1.8 \pm 1.1}$	$\mathbf{-0.07 \pm 0.19 \pm 0.02}$
$\eta_{\gamma\gamma}K_2^{*+}(K^+\pi^0)$	26 ± 12	-1	13	7	2.3	9.1 ± 4.0	-0.16 ± 0.41
$\eta_{3\pi}K_2^{*+}(K^+\pi^0)$	20 ± 8	-1	9	4	2.6	17.8 ± 7.2	-0.82 ± 0.47
$\eta_{\gamma\gamma}K_2^{*+}(K^0_S\pi^+)$	12 ± 10	-1	13	5	1.8	6.4 ± 4.7	0.05 ± 0.58
$\eta_{3\pi}K_2^{*+}(K^0_S\pi^+)$	2 ± 5	$+1$	10	3	0.2	0.9 ± 5.1	-1.00 ± 1.56
$B^+ \to \eta K_2^{*+}(1430)$					**3.5**	$\mathbf{9.1 \pm 2.7 \pm 1.4}$	$\mathbf{-0.45 \pm 0.30 \pm 0.02}$

resonant component. For the parameters of our model [13], 9.6% of the $B \to \eta(K\pi)^*_0$ branching fraction is in the region above $m_{K\pi} = 1535$ MeV where the model is most uncertain. The $K^*_2(1430)$ is generated as a relativistic Breit-Wigner shape with known mass and width [10].

For the signal and $B\bar{B}$ background components we determine the PDF parameters from MC. For background from continuum and nonpeaking combinations from B decays, we obtain the PDF from ($m_{\rm ES}$, ΔE) sideband data for each decay, before applying the fit to data in the signal region; we refine this PDF by letting all parameters vary in the final fit. We parametrize each of the functions $\mathcal{P}_{\rm sig}(m_{\rm ES})$, $\mathcal{P}_{\rm sig}(\Delta E)$, $\mathcal{P}_j(\mathcal{F})$ and the peaking components of $\mathcal{P}_j(m_{\rm res})$ with either a Gaussian, the sum of two Gaussians, or an asymmetric Gaussian function as required to describe the distribution. For $\mathcal{P}_{\rm sig}(\mathcal{H})$ we use a low order polynomial. Slowly varying distributions (all masses, ΔE and $\mathcal{H}$ for continuum background) are represented by one or a combination of linear, quadratic, and phase-space motivated functions [6]. The fitted $q\bar{q}$ background PDF parameters are found to be in close agreement with the initial values. Control samples with topologies similar to our signal modes [e.g., $B \to D(K\pi\pi)\pi$] are used to calibrate the simulated resolutions evaluated from MC [6].

Before applying the fitting procedure to the data we subject it to several tests. In particular, we evaluate possible biases in the yields from our neglect of small residual correlations among discriminating variables in the signal and charmless $B\bar{B}$ background PDFs. The bias is determined by fitting ensembles of simulated $q\bar{q}$ experiments generated from the PDFs into which we have embedded the expected number of signal and $B\bar{B}$ background events, randomly extracted from the fully simulated MC samples. The small biases are listed in Table I. We measure the correlations in the data and find them to be negligibly small.

We compute the branching fraction for each decay by subtracting the fit bias from the measured yield, and dividing the result by the efficiency and the number of produced $B\bar{B}$ pairs. We assume equal decay rates for the $\Upsilon(4S)$ to B^+B^- and $B^0\bar{B}^0$. In Table I we show for each decay mode the measured branching fraction together with the event yield Y_S, efficiency ϵ, and $\mathcal{A}_{\rm ch}$. The significance is taken as the square root of the difference between the value of $-2\ln\mathcal{L}$ (with systematic uncertainties included) for zero signal and the value at its minimum.

For the LMR the measurements for separate daughter decays are combined by adding the values of $-2\ln\mathcal{L}$ as functions of the branching fractions, taking account of the correlated and uncorrelated systematic uncertainties [6] described below.

In Fig. 1 we show projections onto $m_{\rm ES}$ of subsamples enriched with a threshold requirement on the signal likelihood (computed without the variable plotted) that optimizes the sensitivity. There are substantial signals in all

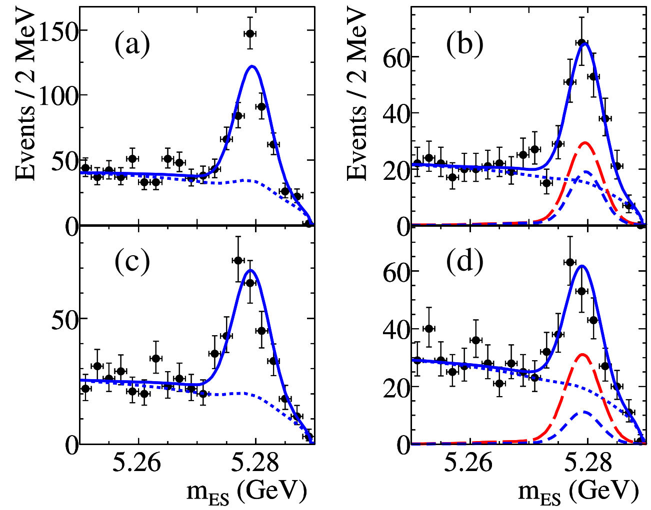

FIG. 1 (color online). B-candidate $m_{\rm ES}$ projections obtained with a cut on the signal likelihood (see text) for (a) $B^0 \to \eta K^{*0}(892)$, (b) $B^0 \to \eta(K\pi)^{*0}_0$ (long-dashed, red) plus $B^0 \to \eta K^{*0}_2(1430)$ (short-dashed, blue), (c) $B^+ \to \eta K^{*+}(892)$, and (d) $B^+ \to \eta(K\pi)^{*+}_0$ (long-dashed, red) plus $B^0 \to \eta K^{*0}_2(1430)$ (short-dashed, blue). Points with uncertainties represent the data, solid curves the full fit functions, and dotted curves the full background functions.

four samples. For the HMR, separation of the $(K\pi)^*_0$ and $K^*_2(1430)$ signals is afforded mainly by the $K\pi$ mass and helicity shapes; projections of these distributions are shown in Fig. 2. The statistical correlations between the two signals are ~ -0.42 in the HMR fits to both the B^0 and B^+ decays.

The largest systematic uncertainties are due to the signal and $B\bar{B}$ PDF modeling, the fit bias correction, the modeling of the $K\pi$ mass distribution, the neutral selection efficiency, and neglect of interference between signal components. The PDF modeling error is largely included in the statistical uncertainty because all background parameters are free in the fit. The uncertainties in the signal PDF parameters are estimated from the consistency of fits to MC and data in control samples with similar final states. Varying the signal PDF parameters within these errors, we estimate the mode-dependent uncertainties to be 1–4 events. The uncertainty in the fit bias correction is taken to be half of the correction. We estimate the uncertainty from modeling the $B\bar{B}$ backgrounds to be less than 1 event.

Uncertainties in the reconstruction efficiency, found from auxiliary studies of inclusive control samples [6], are 0.4% per track, 3.0% per η/π^0, and 1.9% for a K^0_S. Our estimate of the systematic uncertainty for the number of $B\bar{B}$ pairs is 1.1%. Published data [10] provide the uncertainties for the B-daughter product branching fractions (1%–2%). The uncertainty due to the efficiency of the $\cos\theta_T$ requirement is 0.5%. The systematic uncertainty for $\mathcal{A}_{\rm ch}$ is estimated to be 2%, dominated by tracking and PID systematic effects [14].

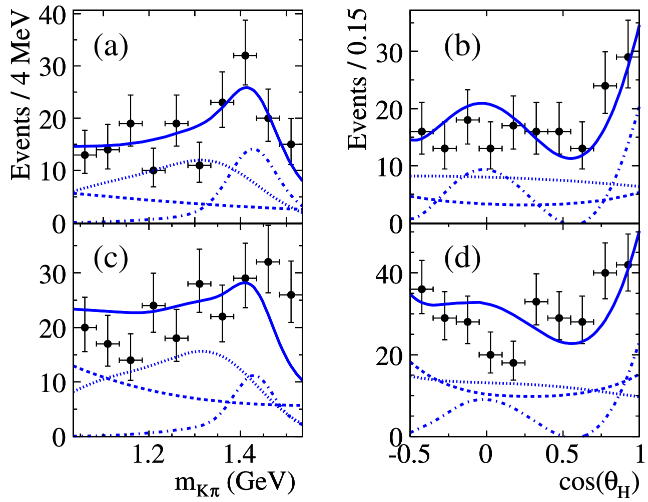

FIG. 2 (color online). Projection of the signals in the HMR, obtained with a cut on the signal likelihood (see text): $K\pi$ mass for (a) B^0, and (c) B^+ channels; $\mathcal{H}$ for (b) B^0, and (d) B^+ channels. Points with uncertainties represent the data, solid curves the full fit functions, dotted curves the $(K\pi)^*_0$ portion, dot-dashed curves the $K^*_2(1430)$ portion, and dashed curves the full background functions.

Because our model does not account for interference among the components, we assign systematic uncertainties based on the $m(K\pi)$ dependence of the complex phases measured in Ref. [12], with allowance for unknown process-dependent overall phases. The effect is small for the LMR and about 10% for the HMR. For the HMR, the systematic uncertainties are applied after the combined fit, taking submode errors as correlated.

In summary, we have presented improved measurements of the branching fractions for the decays $B^0 \to \eta K^{*0}(892)$ and $B^+ \to \eta K^{*+}(892)$, as well as measurements of the decays $B^0 \to \eta(K\pi)^{*0}_0$, $B^+ \to \eta(K\pi)^{*+}_0$, $B^0 \to \eta K^{*0}_2(1430)$, and $B^+ \to \eta K^{*+}_2(1430)$, which had not been seen previously. The first two supersede previous *BABAR* measurements [6] and agree with earlier results and theoretical predictions [1–3]. We also calculate the branching fraction for the resonant decays to $\eta K^*_0(1430)$ using the composition of $(K\pi)^*_0$ from [13]. We find $\mathcal{B}(B^0 \to \eta K^{*0}_0(1430)) = (9.6 \pm 1.4 \pm 0.7 \pm 1.1) \times 10^{-6}$ and $\mathcal{B}(B^+ \to \eta K^{*+}_0(1430)) = (15.8 \pm 2.2 \pm 1.4 \pm 1.7) \times 10^{-6}$, where the third errors arise from the uncertainties on the branching fraction $K^*_0(1430) \to K\pi$ [10] and the resonant fraction of $(K\pi)^*_0$.

There are no theoretical predictions for the decays involving spin-0 or 2 mesons. The measured values of $\mathcal{A}_{\rm ch}$ are mostly consistent with zero within their uncertainties; the value for $B^0 \to \eta K^{*0}(892)$ shows evidence for direct CP violation.

We are grateful for the excellent luminosity and machine conditions provided by our PEP-II colleagues, and for the substantial dedicated effort from the computing organizations that support *BABAR*. The collaborating institutions wish to thank SLAC for its support and kind hospitality. This work is supported by DOE and NSF (U.S.), NSERC (Canada), IHEP (China), CEA and CNRS-IN2P3 (France), BMBF and DFG (Germany), INFN (Italy), FOM (The Netherlands), NFR (Norway), MIST (Russia), MEC (Spain), and PPARC (U.K.). Individuals have received support from the Marie Curie EIF (European Union) and the A. P. Sloan Foundation.

*Also with Università di Perugia, Dipartimento di Fisica, Perugia, Italy
†Also with Università della Basilicata, Potenza, Italy

[1] M. Beneke and M. Neubert, Nucl. Phys. **B675**, 333 (2003).
[2] M.-Z. Yang and Y.-D. Yang, Nucl. Phys. **B609**, 469 (2001); M. Beneke and M. Neubert, Nucl. Phys. **B651**, 225 (2003).
[3] C.-W. Chiang, M. Gronau, and J. L. Rosner, Phys. Rev. D **68**, 074012 (2003); C.-W. Chiang *et al.*, Phys. Rev. D **69**, 034001 (2004).
[4] H. J. Lipkin, Phys. Lett. B **254**, 247 (1991).
[5] S. J. Richichi *et al.* (CLEO Collaboration), Phys. Rev. Lett. **85**, 520 (2000).
[6] B. Aubert *et al.* (*BABAR* Collaboration), Phys. Rev. D **70**, 032006 (2004).
[7] Except as noted explicitly, we use a particle name to denote either member of a charge conjugate pair.
[8] B. Aubert *et al.* (*BABAR* Collaboration), Nucl. Instrum. Methods Phys. Res., Sect. A **479**, 1 (2002).
[9] The use of separate samples for the LMR and HMR limits the number of false combinations among decay products.
[10] S. Eidelman *et al.* (Particle Data Group), Phys. Lett. B **592**, 1 (2004).
[11] The *BABAR* detector Monte Carlo simulation is based on GEANT4: S. Agostinelli *et al.*, Nucl. Instrum. Methods Phys. Res., Sect. A **506**, 250 (2003).
[12] D. Aston *et al.* (LASS Collaboration), Nucl. Phys. **B296**, 493 (1988).
[13] B. Aubert *et al.* (*BABAR* Collaboration), Phys. Rev. D **72**, 072003 (2005); B. Aubert*et al.* (*BABAR* Collaboration) (to be published).
[14] B. Aubert *et al.* (*BABAR* Collaboration), Phys. Rev. Lett. **91**, 171802 (2003).